Preprints.org

Article

Thermally Activated Acoustic Relaxation in Nanostructured and Ultrafine-Grained Titanium

Yuri Semerenko [*] , Vasilij Natsik , Nikolai Galtsov , Diana Hurova , Tamara Bednarchuk , Peter Zinoviev , Viktor Zoryansky , Vladyslav Moskalenko , Ruslan Smolianets , Alexander Smirnov , Yuliya Pohribnaya , Nataly Aksenova

Article

Thermally Activated Acoustic Relaxation in Nanostructured and Ultrafine-Grained Titanium

Yuri Semerenko [1],*, Vasilij Natsik [1], Nikolai Galtsov [1], Diana Hurova [1], Tamara Bednarchuk [2], Peter Zinoviev [1], Viktor Zoryansky [1], Vladyslav Moskalenko [1], Ruslan Smolianets [1], Alexander Smirnov [1], Yuliya Pohribnaya [1] and Nataly Aksenova [3]

[1] B.Verkin Institute for Low Temperature Physics and Engineering of the National Academy of Sciences of Ukraine, 47 Nauky Ave., 61103 Kharkiv, Ukraine

[2] Institute of Low Temperature and Structure Research, Polish Academy of Sciences, P.O. Box 1410, 50-950 Wroclaw, Poland

[3] V.N. Karazin Kharkiv National University, 4 Svobody Sq., 61022 Kharkiv, Ukraine

* Correspondence: semerenko@ilt.kharkov.ua

Abstract

In the range of 5-325 K, the temperature dependence of acoustic properties - absorption and dynamic Young's modulus - was studied in nanocrystalline and fine-crystalline technical purity titanium VT1-0. Measurements were performed using resonance mechanical spectroscopy at 2.4-3.7 kHz. The influence of grain size on low-temperature acoustic behavior was examined. Samples with varying grain sizes were produced by severe plastic deformation through rolling at 100 K and 290 K to true strains of 120-190%, followed by annealing at 525 K, 720 K, and 940 K. Their structures were characterized by electron microscopy and X-ray diffraction. Intense plastic deformation was found to induce an acoustic anomaly, peak P_1, at 150-230 K. Transition from fine- to nanocrystalline states introduced an additional absorption peak, P_2, at 43-78 K. A microscopic dislocation model was proposed to explain these phenomena. The activation parameters of P_1 correspond to thermally activated detachment of dislocation segments from local defects, consistent with the Koiwa-Hasiguti peak. In contrast, the activation parameters of P_2 reflect dislocation motion across a Peierls barrier via thermally activated kink pair formation, analogous to Bordoni peaks observed in fcc crystals. This study demonstrates how grain refinement and deformation strongly affect the acoustic response of titanium, revealing distinct mechanisms of dislocation dynamics at different temperature ranges.

Keywords: nanocryctalline titanium; strength; plasticity; acoustical absorption; dynamical elasticity modulus; cryomechanical treatment

1. Introduction

Currently, there is sustained and growing interest in methods aimed at enhancing the performance characteristics of titanium-based products. This attention is largely driven by titanium's unique combination of high biocompatibility, mechanical strength, and ductility, making it an ideal material for a wide range of engineering and biomedical applications.

One of the conventional approaches to improving the strength of titanium is grain refinement - reducing the grain size down to the nanoscale level (see Figure 1). This strategy is well-established in materials science for its effectiveness in increasing hardness and yield strength through grain boundary strengthening mechanisms (Usmanov et al. 2023 and 2024).
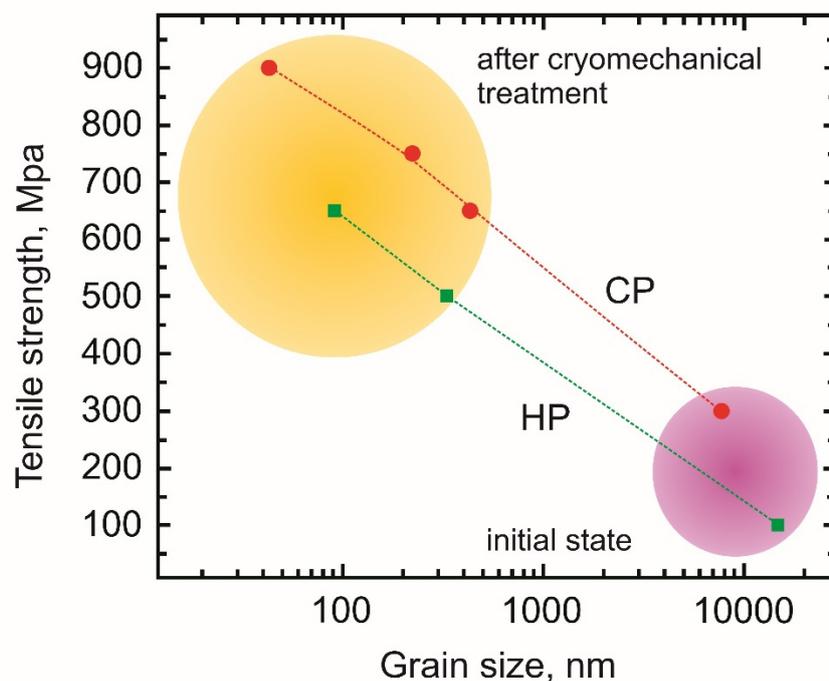
Figure 1. Grain size dependence of the tensile strength of titanium at room temperature. ● - Commercially Pure (CP) titanium VT1-0 (equivalent to ASTM Grade 2); ■ - High-Purity (HP) iodide titanium. The tensile strength of nanostructured commercially pure titanium reaches up to 900 MPa, while that of high-purity titanium approaches 700 MPa. These values are 3 to 5 times higher than those of coarse-grained titanium and are comparable to the strength of coarse-grained alloyed grades (for example Ti6Al4V - Semenova et al. 2005; Zhang et al. 2020).

The figure presents a schematic summary based on data from references (Smirnov and Moskalenko 1994, 2002; Moskalenko and Smirnov 1998; Moskalenko et al. 2005, 2009).

Among several different methods of production, severe plastic deformation is one of the most important and widely used routes; bulk materials with an extremely fine grain structure can be obtained in this way (Valiev et al. 2000).

A particularly promising technique for achieving a nanostructured state in titanium is cryomechanical treatment. This method involves plastic deformation of the material at cryogenic temperatures, which facilitates the formation of ultrafine grains and enhances mechanical properties without compromising ductility (Valiev and Langdon2006, Stolyarov et al. 2003, Semenova et al. 2010). The cryomechanical approach is gaining traction due to its potential for scalable processing and its compatibility with existing manufacturing technologies (Moskalenko et al. 2009).

One of the most effective strategies for tailoring and stabilizing the balance between strength and ductility in titanium subjected to cryomechanical treatment is the application of a subsequent controlled annealing process. This thermal post-treatment enables the relaxation of internal stresses and facilitates partial recovery or recrystallization, depending on the specific parameters employed. By carefully adjusting the annealing temperature and duration, it is possible to fine-tune the microstructural features - such as grain size and dislocation density - thereby optimizing the mechanical performance of the material for targeted applications. Controlled annealing thus plays a crucial role in achieving a desirable combination of high strength and adequate plasticity in nanostructured titanium.

However, the deformation mechanisms in ultrafine-grained metallic materials remain insufficiently understood, particularly with respect to anelastic and microplastic deformation. Mechanical spectroscopy provides a powerful tool for investigating these phenomena. Among its

variants, acoustic spectroscopy stands out as an especially effective method for probing the structural and dislocation-related characteristics of materials.

This technique offers several distinct advantages. Most importantly, it exhibits exceptional sensitivity to microstructural features, enabling the detection and monitoring of subtle processes associated with dislocation dynamics and kinetics. In addition, acoustic spectroscopy is inherently non-destructive, allowing repeated measurements without compromising the integrity of the specimen.

Its high diagnostic capability makes acoustic spectroscopy particularly valuable when employed alongside conventional structural characterization techniques such as X-ray diffraction and electron microscopy. In our earlier studies (Semerenko et al. 2024; Natsik et al. 2025), we demonstrated the effectiveness of this combined approach in tracing the evolution of microstructural states and in providing a more comprehensive understanding of the fundamental mechanisms that govern material behavior.

This study is devoted to examining the influence of controlled annealing and room-temperature aging on the evolution of structural and acoustic properties in NanoCrystalline (grain size 30-50 nm) - NC and Ultrafine-Grained (grain size ~ 1μm) - UFG specimens of commercially pure titanium VT1-0 (contains 0.28% of impurities, including 0.06 wt% of iron, 0.12 wt% of oxigen, 0.02 wt% of nitrogen, 0.01 wt% of carbon and 0.003 wt% of hidrogen; equivalent to ASTM Grade 2). The NC samples were produced via cryomechanical treatment, while the UFG samples were obtained through cold rolling at ambient temperature. By comparing these two processing routes, the research aims to assess how different post-deformation thermal exposures affect microstructural stability, dislocation configurations, and internal friction behavior. Special emphasis is placed on understanding the kinetics of structural relaxation and the sensitivity of acoustic spectroscopy in capturing subtle changes in defect dynamics during thermal and temporal evolution.

2. Experimental Methods

In the temperature range of 5–325 K, the temperature dependences of the logarithmic vibration decrement $\delta(T)$ and the dynamic Young's modulus $E(T)$ were systematically investigated for nanocrystalline and ultrafine-grained commercially pure titanium VT1-0. Acoustic measurements were carried out using the method of resonance mechanical spectroscopy, with electrostatic excitation of the specimen at bending vibration frequencies between 2.4 and 3.7 kHz. The experiments were conducted within the amplitude-independent regime of acoustic strain, ensuring that the observed variations in acoustic properties reflected intrinsic material behavior rather than nonlinear effects associated with large deformation amplitudes. This approach provided reliable insight into the relaxation processes and elastic properties of the nanostructured titanium across a broad cryogenic to room temperature interval.

Linear bending vibrations of a cantilevered specimen were investigated at very small deformation amplitudes, on the order of ε_0 ~ 10⁻⁷. When subjected to a cyclic electric force, the thin plate exhibited forced vibrations, with the excitation frequency f tuned in the vicinity of the fundamental resonant frequency f_r of its mechanical oscillations.

As a consequence, an alternating stress $\sigma = \sigma_0 \sin(\omega t)$ with cyclic frequency $\omega = 2\pi f$ acted upon the material sample. The specimen responded with a small cyclic deformation $\varepsilon_0 \cdot \sin(\omega t - \varphi)$, which - due to the strain viscosity of the sample material - was shifted in phase relative to the applied stress by an angle φ. In this case, $tg\varphi$ is a direct manifestation of the material's internal friction and represents the absorption of mechanical vibration energy within the sample; and the dynamic modulus of elasticity is determined by the deformation component that is in phase with the applied stress.

Thus in this framework, the dynamic modulus of elasticity is defined by the component of the strain that remains in phase with the applied stress, while the out-of-phase component is associated

with energy dissipation. A comprehensive description of the experimental methodology for determining acoustic absorption (internal friction) $Q^{-1}(T)$ and the dynamic Young's modulus $E(T)$ can be found in references (Semerenko 2005; Natsik and Semerenko 2019).

For a cantilevered specimen, the dynamic Young's modulus E and the vibration decrement δ and the associated parameters Q^{-1} are expressed through the following relations:

$$E = 38.3 \frac{\rho l^4}{h^2} \cdot f_r^2 \, , \qquad \delta = \pi Q^{-1} = \pi \frac{|f' - f''|}{f_r} \qquad (1)$$

Here h and l denote the thickness and length of the specimen, respectively, while ρ represents its density (Moskalenko et al. 2014). The parameter $|f' - f''|$ corresponds to the frequency interval in the resonance region within which the amplitude of the forced oscillations decreases to a fraction $\sqrt{2}$ of its resonant value f_r. The magnitude of the numerical coefficient appearing in Equation (1) is determined both by the geometric shape of the specimen and by the value of Poisson's ratio ν.

The non-destructive mechanical spectroscopy method employed in this study combines exceptionally high structural sensitivity, selectivity, and measurement accuracy. The specimens investigated were prepared in the form of thin plates with dimensions of approximately 22×4×0.1-0.3 mm, cut from larger rolled billets to ensure representative microstructural characteristics.

During the course of the acoustic measurements, the temperature was monitored with a precision of 50 mK using a copper-constantan thermocouple, an AsGa thermometer, and a resistive heater to provide fine control. The rate of temperature variation was maintained at approximately 1 K per minute, allowing for stable thermal conditions and reliable acquisition of the mechanical spectroscopy data.

The substructural state of the specimens was produced through severe plastic deformation by rolling at two different temperatures: 100 K, corresponding to Cryogenic Temperature Rolling (CTR); and 290 K, corresponding to Room Temperature Rolling (RTR). The rolling process was carried out to achieve true strain values in the range of e = 1.2÷1.9. The true strain after rolling was determined using the formula $e = \ln\left(\frac{t}{t_0}\right)$, where t and t_0 denote the final and initial thicknesses of the rolled plate, respectively. Following deformation, the samples were subjected to subsequent annealing treatments at 525 K, 720 K, and 940 K in order to investigate the evolution and relaxation of the microstructure.

The long-term stability of the resulting structural state was further assessed by maintaining one of the specimens at ambient conditions for an extended period of seven years. This prolonged exposure at room temperature provided a unique opportunity to evaluate the persistence of the deformation-induced substructure under natural aging conditions.

The method of cryomechanical treatment is grounded in the findings reported in (Moskalenko et al. 1980 and 2009), which examined the fundamental physical mechanisms governing plastic deformation of titanium at cryogenic temperatures. At ambient conditions, plastic deformation of titanium - characterized by its Hexagonal Close-Packed (HCP) crystal structure - proceeds primarily through prismatic slip along $\{10\bar{1}0\}\langle11\bar{2}0\rangle$, with additional contributions from basal $(0001)\langle11\bar{2}0\rangle$ and pyramidal $(0001)\langle11\bar{2}0\rangle$ slip systems, as well as mechanical twinning, most commonly of the $\{10\bar{1}2\}$ and $\{11\bar{2}2\}$ types.

When deformation occurs at low temperatures, mechanical twinning assumes a far more dominant role as a complementary mode of plasticity. In fact, nearly all grains within a polycrystalline aggregate undergo twinning even at relatively small strains. This behavior is facilitated by the wide variety of twinning systems that become active under cryogenic conditions,

together with the enhanced propensity for twinning itself. Both extension twins (e.g., $\{11\bar{2}2\}$ and $\{10\bar{1}2\}$), which elongate crystallites (grain) along the c-axis, and compression twins (e.g., $\{11\bar{2}2\}$ and $\{11\bar{2}4\}$), which shorten grains along the *c*-axis, are observed.

The simultaneous activation of multiple twinning systems leads to pronounced grain refinement. Moreover, additional fragmentation of grains arises from the extensive development of secondary and tertiary twinning, the intersection of twin boundaries, twinning within accommodation zones at the twin - matrix interface, and interactions between twins and grain boundaries. Collectively, these processes produce a highly refined microstructure, underscoring the unique effectiveness of cryomechanical treatment in generating nanostructured states in titanium.

A more detailed description and justification of the cryorolling method applied to titanium is provided in (Moskalenko et al. 2009). In that work, the principles of low-temperature plastic deformation are discussed comprehensively, with particular emphasis on the mechanisms of grain refinement, defect generation, and the stabilization of nanostructured states. The methodology is substantiated both theoretically and experimentally, demonstrating how cryogenic rolling not only enhances the strength of titanium but also preserves its ductility by suppressing dynamic recovery processes.

Transmission Electron Microscopy (TEM) investigations revealed that the intragranular substructure of titanium deformed at 290 K is characterized by dense dislocation accumulations. These clusters give rise to numerous bending extinction contours (Figure 2a), which are indicative of a high level of internal stresses. The size of such regions ranges from fractions of a micron to several microns. In contrast, the substructure of cryogenically deformed material is dominated by Coherent Scattering Regions (CSR) with dimensions of approximately 30-50 nm (Figure 2b). After cryogenic deformation to a true strain of e = 1.2, CSR are observed primarily in the form of clusters. With increasing strain, these clusters gradually disintegrate, and the CSR become more uniformly distributed throughout the microstructure.
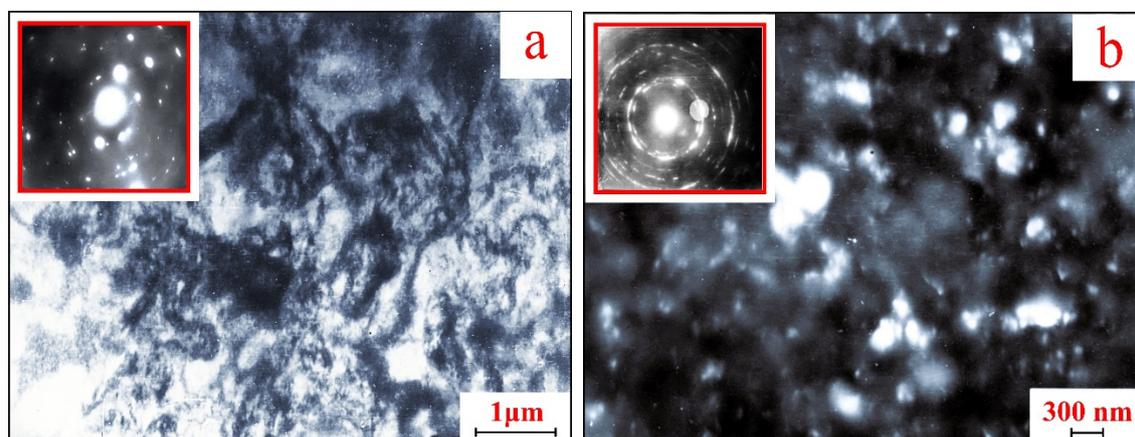

Figure 2. Dark-field transmission electron microscopy (TEM) image of commercially pure titanium VT1-0 after plastic deformation to a true strain of e = 1.8: (a) specimen rolled at 290 K (RTR), and (b) specimen rolled at 100 K (CTR).

The genesis of CSR is attributed to repeated twinning processes occurring in titanium under conditions of low-temperature deformation (Moskalenko et al. 1980). This mechanism provides a consistent explanation for the formation and evolution of nanoscale structural features in cryogenically rolled titanium. The structure of nanocrystalline titanium VT1-0, produced by low-temperature deformation, has been thoroughly investigated in earlier studies (Moskalenko et al. 1980, 2009, 2014) using bright-field and dark-field transmission electron microscopy as well as X-ray diffraction analysis. These complementary techniques provided detailed insight into the microstructural features, including grain refinement, defect distribution, and the evolution of CSRs,

thereby establishing a comprehensive picture of the nanoscale architecture of cryogenically deformed titanium.

The evolution of the histograms of CSR size distributions in the VT1-0 titanium specimen after CTR to a true strain of e = 1.9 and subsequent annealing at 525 K and 720 K is presented in Figure 3. It is clearly seen that cryomechanical processing of titanium leads to pronounced grain fragmentation, resulting in an average CSR size of approximately 36 nm. Annealing at 525 K produces only a slight increase in the mean crystallite size, raising it to about 43 nm. At the same time, annealing at this temperature almost completely relieves the internal stresses introduced into the material during cryorolling. Further annealing at 720 K causes a twofold increase in the average grain size, reaching ~70 nm. Finally, annealing at 940 K induces full recrystallization, leading to the disappearance of the nanostructured state of the specimens.

X-ray studies of the samples structure were carried out on a DRON-2 serial diffractometer in radiation of a copper anode with a nickel filter at room temperature by scanning following the scheme $\theta - 2\theta$ with collimating slits (Braude et al. 2011). The scattering intensity was recorded over the angular range $4° < 2\theta < 140°$ in continuous mode with automated computer acquisition.
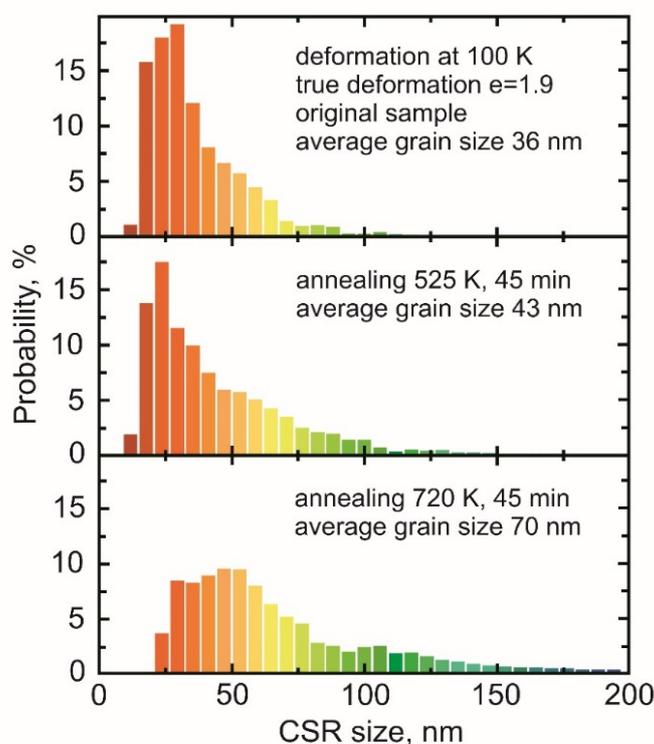
Figure 3. Histograms illustrating the distribution of crystallite sizes (Coherent Scattering Regions, CSR) in the VT1-0 titanium specimen after cryogenic deformation to a true strain of e = 1.9 and subsequent annealing treatments.

Structural parameters were evaluated by analyzing the intensity, profile shape, and the width of the diffraction reflections. The determination of size L of regions with X-ray coherent scattering in crystallites and of a level of microdeformations $\Delta \varepsilon$ was performed by means of approximation method via widening diffraction maxima (Williamson and Hall 1953, Williamson and Smallman 1956, Patterson 1939). The contribution to the dislocation density calculated from the particle size ρ_L, as well as the total average dislocation density $\langle \rho \rangle$ was determined using an approximation method based on the broadening of diffraction maxima, following the procedure described in (Semerenko et al. 2025 and Natsik et al. 2025). The calculation of ρ_ε for the hexagonal lattice was

performed using the method proposed by (Malykhin et al. 2009). Table 1 summarizes the results of X-ray diffraction patterns processing in different structural states.

Table 1. Structural parameters of the VT1-0 titanium specimen after CTR from X-ray diffraction. The size L of regions exhibiting X-ray coherent scattering in crystallites, as well as the level of microdeformation $\Delta\varepsilon$ and the unit cell parameters were taken from (Plotnikova et al. 2016 и 2017).

e	L, nm	$\Delta\varepsilon\ 10^{-3}$	parameters cell		$\rho_L\ 10^{14}$, m^{-2}	$\rho_\varepsilon\ 10^{14}$, m^{-2}	$\langle\rho\rangle\ 10^{14}$, m^{-2}
			a, Å	c, Å			
0	282	0.6	2.958	4.711	0.37	0.15	0.23
0.12	182	2.3	2.964	4.699	0.9	2.13	1.39
0.6	110	0.3	2.998	4.729	2.48	0.04	0.3
1.2	55	3.9	2.967	4.709	9.9	6.1	7.78
2	64	3.8	2.972	4.709	7.32	5.78	6.51

In (Braude et al. 2011) it is shown that X-ray investigations reveal the presence of an X-ray amorphous phase; however, crystallites smaller than 15 nm cannot be distinguished from an amorphous phase by X-ray diffraction, whereas TEM makes it possible to differentiate a true amorphous phase and directly observe crystallites of any size. A comparison of titanium after CTR and RTR rolling demonstrated a 10% higher content of the X-ray amorphous phase under low-temperature deformation, accompanied by strong diffuse scattering characteristic of distorted crystals. It should be noted, however, that TEM provides local information on the morphology and distribution of crystallites, while X-ray diffraction delivers integral data over large sample volumes, including the evaluation of microstresses, texture, and lattice parameters.

3. Results and Discussion

The formation of deformation-induced microstructures, both in nanocrystalline (CTR) and ultrafine-grained (RTR) titanium, gives rise to the appearance of an acoustic relaxation peak, denoted as P₁, in the temperature dependence of the logarithmic vibration decrement $\delta(T)$ at approximately 230 K (see Figures 4). In the corresponding temperature dependence of the dynamic Young's modulus $E(T)$ this peak manifests itself as a broadened step, the center of which coincides with the temperature of the absorption maximum. A similar relaxation process in VT1-0 titanium was also reported by other authors following Severe Plastic Deformation (SPD) by rolling at room temperature (Kardashev 2017).

An increase in the degree of plastic deformation leads to both a broadening and an enhancement of the amplitude of the P₁ absorption peak. In nanocrystalline specimens (CTR), the amplitude of P₁ is significantly higher than in ultrafine-grained (RTR) samples, reflecting the stronger contribution of the nanostructured state to relaxation phenomena. A series of annealing treatments at 525 K, 720 K, and 940 K progressively reduces the height of the P₁ peak and shifts its localization temperature, eventually leading to its disappearance.

It should be emphasized that the P₁ peak is considerably broader than the classical Debye peak and exhibits a pronounced frequency dependence. With increasing resonance frequency of the mechanical vibrations of the specimen, the peak shifts toward higher temperatures, thereby confirming its thermally activated character.

The red line in Figure 4b corresponds to storage after CTR at room temperature for 7 years.

The temperature dependences of $\delta(T)$ are shown after subtraction of the background absorption δ_{BG}, which is defined by relation (8).
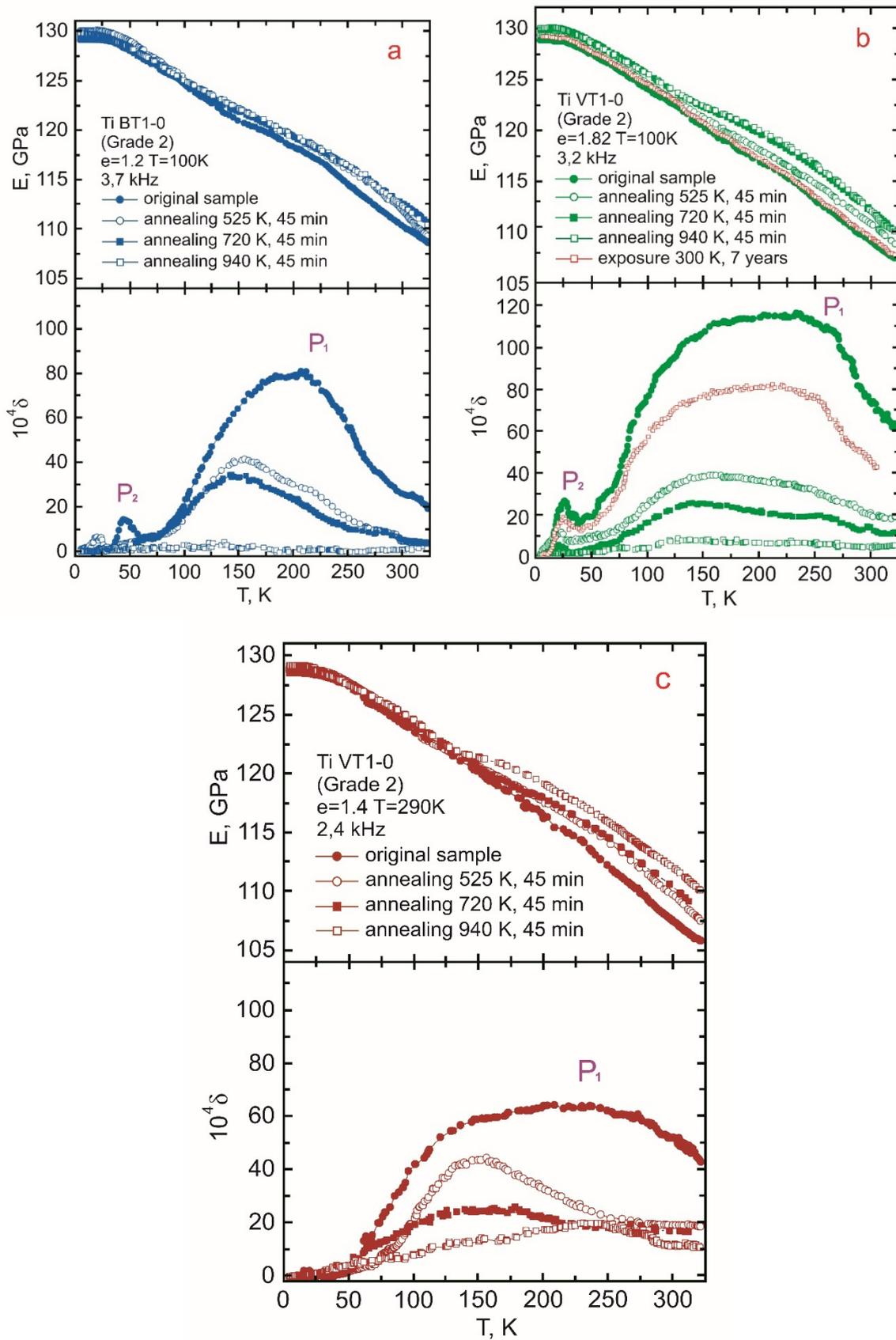
Figure 4. 4a and 4b Temperature dependences of the logarithmic decrement of oscillations $\delta(T)$ and the dynamic Young's modulus $E(T)$ of commercially pure titanium VT1-0 after CTR at different levels of cryogenic deformation: a) e = 1.2, b) e = 1.82. Immediately after CTR, as well as after a series of successive anneals. c

Temperature dependences of the logarithmic decrement of oscillations $\delta(T)$ and the dynamic Young's modulus $E(T)$ of commercially pure titanium VT1-0 after rolling at room temperature at deformation e = 1.4.

Immediately after RTR, as well as after a series of successive anneals.

The temperature dependences of $\delta(T)$ are shown after subtraction of the background absorption δ_{BG}, which is defined by relation (8).

The temperature dependence of the vibration decrement $\delta(T)$ in the region of the P₁ peak can be satisfactorily described within the framework of the theory of statistically broadened, thermally activated relaxation resonance. In this approach, the distribution function of activation energies is assumed to be of a quasi-Gaussian type with a small dispersion D (Natsik and Semerenko 2004, 2016):

$$\delta(T) = C_r \Delta_0 F_1(\theta, \Omega, d), \qquad F_1 = \frac{2\Omega\theta^2}{\sqrt{\pi}d\ln\Omega}\int_1^\infty dx \frac{\ln x}{x^2 + \Omega^2}\exp\left[-\left(\frac{\theta\ln x - \ln\Omega}{d}\right)^2\right] \qquad (2)$$

where $\Omega = \dfrac{1}{\omega\tau_0}$, $\theta = \dfrac{kT\ln\Omega}{U_0}$, $d = \dfrac{\sqrt{2}D}{U_0}\ln\Omega$; ω is the cyclic frequency of oscillations, k is the Boltzmann constant, τ_0 is the attempt period, and U_0 is the activation energy.

This formalism provides a consistent description of the observed relaxation behavior, capturing both the frequency dependence and the thermal activation character of the P₁ peak. The quasi-Gaussian distribution reflects the statistical nature of defect - dislocation interactions, while the small dispersion ensures that the resonance remains well localized in temperature space.

It is well established that the total deformation of a real crystal under mechanical loading consists of both elastic and inelastic components. The fundamental distinction between them lies in the fact that elastic deformation occurs instantaneously, whereas inelastic deformation exhibits a certain time dependence governed by relaxation processes. Because of the presence of this relaxing component, it is customary to distinguish between two limiting values of the elastic modulus. The first is the quasi-static, unrelaxed modulus E_U, which characterizes the immediate response of the crystal to loading in the absence of any inelastic contribution. The second is the relaxed modulus E_R, measured after a time interval much longer than the characteristic relaxation times of all processes relevant within the studied temperature range. When the crystal is subjected to a periodic load with cyclic frequency ω, its mechanical properties are determined by the dynamic modulus of elasticity $E_{\exp}(T,\omega)$; in this case $E_R < E_{\exp}(\omega,T) < E_U$ and there exists a certain defect of the modulus which reflects the contribution of relaxation phenomena to the overall elastic response of the material.

In general, the dynamic modulus of elasticity depends on both temperature T and frequency ω. Following (Natsik and Semerenko 2019), we will assume that the temperature-frequency dependence of the dynamic elasticity modulus $E_{\exp}(T,\omega)$ recorded in experiments can be divided into resonant $E_R(T,\omega)$ and background $E_{BG}(T,\omega)$ components:

$$E_{\exp}(T,\omega) = E_0(\omega) - E_{BG}(T,\omega) - E_R(T,\omega) \qquad (3)$$

where $E_0(\omega)$ is the limit value of the module at $T \to 0$ and the value of the parameter E_0 is close to the value of the static modulus of elasticity of a dislocation-free crystal.

In general case the background component $E_{BG}(T,\omega)$ is mainly determined by the interaction of elastic vibrations with thermal phonons end electrons. For the Debye model of the phonon spectrum with a characteristic Debye temperature Θ_D, the softening of the elastic modulus by phonons and electrons is described by the formula:

$$\frac{E_{BG}(T,\omega)}{E_0(\omega)} = M_1 \cdot f\left(\frac{T}{\Theta_D}\right) + M_2 \cdot T^2, \qquad (4)$$

where $M_1 \cdot f\left(\dfrac{T}{\Theta_D}\right)$ is the phonon-induced modulus defect; $M_2 \cdot T^2$ is the modulus defect caused

by the thermal motion of conduction electrons; $f\left(\dfrac{T}{\Theta_D}\right) = \left(\dfrac{T}{\Theta_D}\right)^4 \cdot \displaystyle\int_0^{\frac{\Theta_D}{T}} dx \, \dfrac{x^3}{e^x - 1}$. Then:

$$E_{\exp}(T, \omega) = E_0(\omega) \cdot \eta(T) - E_R(T, \omega), \qquad \eta(T) = 1 - M_1 \cdot f\left(\dfrac{T}{\Theta_D}\right) - M_2 \cdot T^2 \qquad (5)$$

Temperature dependence of the resonant component of the Young's modulus

$$E_R(T, \omega) = E_0(\omega) \cdot \eta(T) - E_{\exp}(T, \omega) \qquad (6)$$

In our case, the contribution of the relaxation process under investigation to the defect component of the elastic modulus is well described within the framework of the theory of statistically broadened, thermally activated relaxation resonance (Natsik and Semerenko 2004, 2016):

$$E_R(T, \omega) = \dfrac{C_r \Delta_0}{\pi} F_2(\theta, \Omega, d), \qquad F_2 = \dfrac{2\Omega^2 \theta^2}{\sqrt{\pi} d \ln \Omega} \int_1^\infty dx \, \dfrac{\ln x}{x} \dfrac{1}{x^2 + \Omega^2} \exp\left[-\left(\dfrac{\theta \ln x - \ln \Omega}{d}\right)^2\right] \qquad (7)$$

This theoretical approach accounts for the distribution of activation energies and the statistical nature of defect interactions, thereby providing a consistent explanation of the observed behavior. By considering the resonance as a thermally activated process with a broadened spectrum, the model captures both the energy absorption and the elastic response of the nanostructured titanium, offering a reliable description of the relaxation phenomena detected in the experiments.

The estimated activation parameters of the P_1 relaxation peak - namely, an activation energy of $U_0 \approx 0.38$ eV and an attempt period of $\tau_0 \approx 2 \cdot 10^{-13}$ s are in good agreement with the values previously reported in (Hasiguti et al. 1962; Golovin et al. 2006).

The overall set of properties associated with the P_1 peak strongly suggests its dislocation-deformation origin. Moreover, the pronounced structural sensitivity of the system of relaxators responsible for the emergence of this peak highlights the intimate connection between microstructural features and relaxation behavior in nanocrystalline titanium. This interpretation reinforces the view that the P_1 peak reflects the collective dynamics of dislocations interacting with the defect landscape of the material. Such peaks are generally linked to dislocation dynamics and the interaction of lattice defects with stress fields, thereby providing valuable insight into the relaxation mechanisms operating in the nanostructured material. The differences in the microstructural features formed at 100 K and 290 K, arising from distinct deformation mechanisms, indicate that this relaxation resonance is not directly associated with the intragranular microstructure. The experimentally determined activation parameters are typical of the so-called Koiwa - Hasiguti peaks (Koiwa and Hasiguti 1965), which are linked to the process of thermally activated detachment of a dislocation segment from a local structural defect. Such defects may include impurity atoms, interstitials, or vacancies.

In this interpretation, U_0 represents the activation energy required for detachment, while τ_0 corresponds to the oscillation period of the dislocation segment that interacts directly with the defect. This framework provides a consistent explanation of the observed relaxation behavior and highlights the role of defect - dislocation interactions in the mechanical response of cryogenically and room-temperature deformed titanium.

With increasing temperature, a pronounced growth of the background absorption δ_{BG} is observed. Considering the strong temperature sensitivity of the background absorption, it can be attributed in part to non-conservative viscous dislocation motion (Schoeck et al. 1964). This process is characterized by an activation energy U_{BG}, which differs from that governing the internal-friction mechanism. Such behavior indicates that background absorption originates from an independent

relaxation channel, reflecting the complex interaction between dislocation dynamics and defect structures in nanocrystalline titanium. The non-conservative nature of dislocation motion enhances energy dissipation, while the variation in activation energies points to multiple thermally activated mechanisms shaping the material's acoustic response;

$$\delta_{BG} = A_1 + A_2 \exp\left(-\frac{U_{BG}}{kT}\right) \tag{8}$$

where the coefficients A_1 and A_2 are fitting parameters, whose values vary with changes in the defect structure of the sample.

Cryogenically deformed (CTR) specimens exhibit a number of distinctive features (see Figures 4a and 4b).

First, in the temperature range of 43-78 K, a relaxation peak of acoustic absorption, denoted as P_2, is observed. Increasing the degree of cryodeformation leads to a narrowing of the P_2 peak and a shift of its localization temperature to lower values. Annealing at 525 K reduces both the height and the localization temperature of the P_2 peak, while after annealing at 720 K the P_2 peak is practically absent.

The absorption peak P_2 also exhibits a pronounced frequency dependence: with increasing frequency of mechanical oscillations, the peak shifts toward higher temperatures, confirming its thermally activated nature. Estimates of the activation parameters of the P_2 peak: the activation energy of $U_0 \approx 0.03$ eV and an attempt period of $\tau_0 \approx 2 \cdot 10^{-11}$ s.

This behavior highlights the sensitivity of the P_2 resonance to both structural state and external conditions, emphasizing its origin in defect - dislocation interactions that are strongly influenced by cryogenic deformation and subsequent thermal treatment.

A comparable absorption peak, interpreted within the framework of dislocation relaxation mechanisms of the Bordoni type, had previously been recorded in deformed coarse-grained commercially pure titanium (Miyada et al. 1977). This earlier observation underscores the universality of Bordoni-type relaxation phenomena, which manifest not only in nanostructured states but also in conventional coarse-grained materials. The presence of such a peak in technically pure titanium highlights the fundamental role of dislocation dynamics in governing internal friction, regardless of grain size or processing route.

Such values of the activation parameters are characteristic of the process in which dislocations overcome the Peierls relief through the thermally activated nucleation of paired kinks. In other words, this relaxation peak can be regarded as analogous to the Bordoni peaks typically observed in Face-Centered Cubic (FCC) crystals (Seeger 1956; Seeger and Shiller 1964; Seeger and Wüthrich 1976). This analogy highlights the fundamental role of dislocation dynamics in the observed relaxation behavior: the kink-pair mechanism provides a pathway for dislocations to surmount lattice resistance, thereby producing a distinct internal friction peak. The similarity to Bordoni peaks in FCC metals underscores the universality of this mechanism across different crystal structures, even in nanostructured titanium. It should be noted that a relaxation peak analogous to P_2 was also observed in nanostructured zirconium (Vatazhuk et al. 2011), produced by severe plastic deformation. This finding underscores the universality of such relaxation phenomena in hexagonal close-packed metals subjected to intensive grain refinement, and highlights the close connection between dislocation - defect interactions and the emergence of thermally activated acoustic peaks.

Secondly, in cryogenically deformed (CTR) specimens in the nanostructured state, the dynamic Young's modulus E is reduced by approximately $\Delta E \approx 0.8\text{-}1.2\%$ compared to the same specimens after recrystallization annealing at 940 K. Moreover, the magnitude of ΔE increases with the degree of cryodeformation. Annealing at 525 K decreases ΔE, while subsequent annealing at 720 K causes the low-temperature portions of the $E(T)$ curves for cryodeformed and recrystallized samples to nearly coincide.

This behavior of the modulus is most likely associated with the formation and subsequent evolution of the nanostructured state (Valiev et al. 2013, 2024). The observed reduction in modulus

reflects the sensitivity of elastic properties to nanoscale grain refinement and defect structures, while the progressive recovery during annealing highlights the role of structural relaxation and grain growth in restoring the mechanical response of titanium.

These characteristics reflect the profound influence of low-temperature plastic deformation on the microstructural state of titanium, including enhanced grain refinement, increased density of defects, and the activation of multiple twinning systems. As a result, the mechanical and relaxation properties of cryodeformed samples differ markedly from those of conventionally deformed or recrystallized materials, underscoring the unique role of cryomechanical processing in stabilizing nanostructured states.

4. Conclusions

1. The temperature dependences of the logarithmic vibration decrement $\delta(T)$ and the dynamic Young's modulus $E(T)$ have been systematically investigated for nanostructured and ultrafine-grained titanium VT1-0 of technical purity. These measurements provide direct insight into the relaxation phenomena and elastic behavior of titanium subjected to cryogenic deformation and subsequent annealing, thereby revealing the strong influence of microstructural refinement on the mechanical response of the material.

2. It has been established that severe plastic deformation by rolling leads to pronounced grain fragmentation in the initial titanium material. In the substructure of specimens deformed at 100 K, coherent scattering regions (CSR) with dimensions of approximately 30-50 nm predominate. In contrast, after deformation at 290 K, the CSR size ranges from fractions of a micron to several microns.

This clear distinction highlights the strong influence of deformation temperature on the mechanisms of microstructural refinement. Cryogenic rolling promotes the formation of nanoscale domains due to the activation of multiple twinning systems, whereas deformation at room temperature results in comparatively coarser substructures. Such temperature-dependent behavior underscores the critical role of low-temperature processing in achieving and stabilizing nanostructured states in titanium.

3. Severe plastic deformation gives rise to a relaxation resonance, denoted as P_1, at a temperature of approximately 230 K. The activation parameters of this peak are estimated as an activation energy of $U_0 \approx 0.38$ eV and an attempt period of $\tau_0 \approx 2 \cdot 10^{-13}$ s.

The overall set of properties associated with the P_1 resonance allows it to be attributed to the Koiva - Hasiguti relaxation process. This mechanism involves the thermally activated detachment of dislocation segments from local structural defects, such as impurity atoms, interstitials, or vacancies, and is a well-established source of internal friction peaks in hexagonal close-packed metals. The identification of with this relaxation process underscores the strong role of defect-dislocation interactions in shaping the acoustic and elastic response of cryogenically deformed titanium.

4. The formation of a nanostructured state during cryogenic deformation is accompanied by a reduction in the dynamic Young's modulus by approximately $\Delta E \approx 0.8\text{-}1.2\%$ across the entire investigated temperature range. Moreover, the magnitude of ΔE increases with the degree of cryodeformation. Recrystallization annealing at 940 K restores the modulus to its original values.

This behavior reflects the strong sensitivity of the elastic properties of titanium to nanoscale grain refinement and defect accumulation. The reduction in modulus can be attributed to the enhanced density of dislocations and twin boundaries generated during cryogenic rolling, while the recovery of the modulus upon high-temperature annealing highlights the role of structural relaxation and grain growth in eliminating these defects and re-establishing the equilibrium microstructure.

5. The nanostructured state of the specimens is characterized by the presence of a relaxation peak, denoted as P_2, observed in the temperature range of 43–78 K. This peak is associated with an activation energy of approximately $U_0 \approx 0.03$ eV and an attempt period of $\tau_0 \approx 2 \cdot 10^{-11}$ s. The combination of its properties indicates that the P_2 peak is analogous to the Bordoni peaks typically observed in Face-Centered Cubic (FCC) crystals.

Data Availability Statements: The authors declare that the data supporting the findings of this study are available within the papers: https://doi.org/10.1016/0001-6160(65)90032-5, https://doi.org/10.1063/1.3266928, https://doi.org/10.1016/0956-7151(94)90114-7, https://doi.org/10.1016/S0921-5093(97)00713-2, https://doi.org/10.1063/1.2126949, https://asm.matweb.com/search/SpecificMaterial.asp?bassnum=MTP641, https://www.azom.com/properties.aspx?ArticleID=1547, https://doi.org/10.2320/matertrans.46.2020.

References

Braude IS, Gal'tsov NN, Moskalenko VA, Smirnov AR (2011) Investigation of titanium nanostructure deformed at low temperatures. Low Temp. Phys. 37(12):1042-1048. https://doi.org/10.1063/1.3674268

Golovin IS, Pavlova TS, Golovina SB, Sinning HR, Golovin SA (2006) Internal friction and microplasticity in ultrafine-grained copper produced by severe plastic deformation. Mater. Sci. Eng. A 442(1-2):165-169. https://doi.org/10.1016/j.msea.2006.01.109

Hasiguti RR, Igata N, Kamoshita G (1962) Internal friction peaks in cold-worked metals. Acta Metall. 10(4):442-447. https://doi.org/10.1016/0001-6160(62)90023-8

Kardashev BK, Sapozhnikov KV, Betekhtin VI, Kadomtsev AG, Narykova MV (2017) Internal friction, Young's modulus, and electrical resistivity of submicrocrystalline titanium. Phys. Solid State 59(12):2381-2386. https://doi.org/10.1134/S1063783417120204

Koiwa M and Hasiguti RR (1965). A theory of internal friction peak due to thermal unpinning of dislocations and its application to P1 peak in copper. Acta Metall. 13(12):1219-1230. https://doi.org/10.1016/0001-6160(65)90032-5

Malykhin DG, & Korneeva VV (2009) X-ray study of defect structures in titanium (*in Ukrainian*). Visnyk of V. N. Karazin Kharkiv National University. Series: Nuclei, Particles, Fields, 859:83-88. Retrieved from http://nuclear.univer.kharkov.ua

Miyada LT, Watanabe S, Tanaka K, Isore A (1977) Internal friction peaks in cold-worked and irradiated titanium. Phys. Status Solidi A42(2):235-242. https://doi.org/10.1002/pssa.2210420125

Moskalenko VA, Startsev VI, Kovaleva VN (1980) Low temperature peculiarities of plastic deformation in titanium and its alloys. Cryogenics 20(9):507–512.

Moskalenko VA and Smirnov AR (1998) Temperature effect on formation of reorientation bands in α- Ti. Mater. Sci. Eng. A46(1-2):282-288. https://doi.org/10.1016/S0921-5093(97)00713-2

Moskalenko VA, Natsik VD, Kovaleva VN (2005) The role of Peierls relief in the low-temperature plasticity of pure α-Ti. Low Temp. Phys. 31(10):907-914. https://doi.org/10.1063/1.2126949

Moskalenko VA, Smirnov AR, Moskalenko AV (2009). Nanocrystalline titanium produced by the cryomechanic method: Microstructure and mechanical properties. Low Temp. Phys. 35(11):905-907. https://doi.org/10.1063/1.3266928

Moskalenko VA, Betekhtin VI, Kardashev BK et al. (2014) Mechanical properties and structural features of nanocrystalline titanium produced by cryorolling. Phys. Solid State **56**, 1590-1596. https://doi.org/10.1134/S1063783414080204

Natsik VD and Semerenko YuA (2004) Analysis of low-temperature relaxation resonances in materials containing defects. Funct. Mater. 11(2):327-333. Retrieved from http://dspace.nbuv.gov.ua/handle/123456789/138820

Natsik VD and Semerenko YuA (2016) Dislocation mechanisms of low-temperature internal friction in nanostructured materials. Low Temp. Phys. 42:138-148. https://doi.org/10.1063/1.4942907

Natsik VD and Semerenko YA (2019) Dislocation mechanisms of low-temperature acoustic relaxation in iron. Low Temp. Phys. 45(5):551-567. https://doi.org/10.1063/1.5097366

Natsik V, Semerenko Y, Galtsov N, Hurova D, Zoryansky V, Tabachnikova E, Bednarchuk T, Zinoviev P. (2025) Analysis of the dislocation structure, kinetics and dynamics in the high-entropy alloy $Al_{0.5}CoCrCuFeNi$. Eng. Innov. 15:1-8. https://doi.org/10.4028/p-V4p5sx

Patterson A (1939) The Scherrer formula for X-Ray particle size determination. Phys. Rev. 56:978-982. https://doi.org/10.1103/PhysRev.56.978Plotnikova YuM, Braude IS, & Moskalenko VA (2016) X-ray parameters of a nanocrystalline titanium microstructure, obtained via cryodeformation. Low Temp. Phys. 42(12), 1175-1180. https://doi.org/10.1063/1.4973594

Plotnikova YuM, Smolianets RV, Braude IS, & Moskalenko VA (2017) X-ray parameters of nanocrystalline titanium microstructure produced by cryodeformation. East Eur. J. Phys. 4(1):56-61. https://doi.org/10.26565/2312-4334-2017-1-04

Schoeck G, Bisogni E, Shyne J (1964) The activation energy of high temperature internal friction. Acta Metall. 12(12):1466-1468. https://doi.org/10.1016/0001-6160(64)90141-5

Seeger A (1956) On the theory of the low-temperature internal friction peak observed in metals. Phil. Mag. 1(7):651-662. https://doi.org/10.1080/14786435608244000

Seeger A and Shiller P (1964) Kinks in dislocation lines and their effects on the internal friction in crystals.   W.P. Mason (Ed.) Physical Acoustics Vol III (A). Academic Press, New York.

Seeger A and Wüthrich C (1976) Dislocation relaxation processes in body-centred cubic metals. Nuov. Cim B 33:38-75. https://doi.org/10.1007/BF02722472

Semenova IP, Valiev RZ, Yakushina EB, Lowe TC (2005). Mechanical properties of ultrafine-grained Ti-6Al-4V alloy processed by severe plastic deformation. Mater. Trans. 46(9):2020-2025. https://doi.org/10.2320/matertrans.46.2020

Semenova IP, Polyakov AV, Valiev RZ (2010) Nanostructured titanium for biomedical applications produced by cryomechanical treatment. Mater. Sci. Forum 633-634:795-804. https://doi.org/10.4028/www.scientific.net/MSF.633-634.795

Semerenko YuA (2005) Interfacing the Instrumental GPIB with a Personal Computer Through the LPT Port. Instrum. Exp. Tech. 48:608-610. https://doi.org/10.1007/s10786-005-0107-x

Semerenko YO, Natsik VD, Tabachnikova ED, Huang Y, Langdon TG (2024) Mechanisms of low-temperature dislocation motion in high-entropy $Al_{0.5}CoCrCuFeNi$ alloy. Metals 14(7):778-798. https://doi.org/10.3390/met14070778

Semerenko Yu, Natsik V, Galtsov N, Hurova D, Zoryansky V, Tabachnikova E, Bednarchuk T, Kolodiy I, Zinoviev P (2025) Investigation of Structure of the High-Entropy Alloy $Al_{0.5}CoCrCuFeNi$, Adv. Mater. Sustain. Manuf. 2(3): 10012. https://doi.org/10.70322/amsm.2025.10012

Smirnov AR and Moskalenko VA (1994) Low-temperature deformation of titanium and the formation of a nanocrystalline structure. Acta Metall. Mater. 42(8):2603-2610. https://doi.org/10.1016/0956-7151(94)90114-7

Smirnov AR. and Moskalenko VA (2002) Low-temperature plasticity and internal friction in α-Ti single crystals. Mater. Sci. Eng. A327(1):138-143. https://doi.org/10.1016/S0921-5093(01)01613-7

Stolyarov VV, Zhu YT, Alexandrov IV, Lowe TC, Valiev RZ (2003) Grain refinement and enhanced mechanical properties in titanium processed by cryogenic severe plastic deformation. Mater. Sci. Eng. A 343(1-2):43-50. https://doi.org/10.1016/S0921-5093(02)00293-6

Usmanov EI, Rezyapova LR, Valiev RZ (2023) High-strength state and strengthening mechanisms of ultrafine-grained titanium. Phys. Mesomech. 26(5):483-494. https://doi.org/10.1134/S1029959923050016

Usmanov EI, Gutkin MY, Wu Y, Sha G, Valiev RZ (2024) Superstrength of nanostructured Ti Grade 4 with grain boundary segregations. Metals 15(6):618. https://doi.org/10.3390/met15060618

Valiev RZ, Islamgaliev RK, Alexandrov IV (2000) Bulk nanostructured materials from severe plastic deformation. Prog. Mater. Sci. 45(2):103-189. https://doi.org/10.1016/S0079-6425(99)00007-9

Valiev RZ, Langdon TG (2006) Principles of equal-channel angular pressing as a processing tool for grain refinement. Prog. Mater. Sci. 51(7):881-981. https://doi.org/10.1016/j.pmatsci.2006.02.001

Valiev RZ, Zhilyaev AP, Langdon TG (2013) Bulk Nanostructured Materials: Fundamentals and Applications. John Wiley & Sons.

Valiev RZ, Alexandrov IV, Kawasaki M, Langdon TG (2024) Ultrafine-Grained Materials. Springer.

Vatazhuk EN, Pal-Val PP, Natsik VD, Pal-Val LN, Tikhonovsky MA, Velikodny AN, Khaimovich PA (2011) Low-temperature acoustic properties of nanostructured zirconium obtained by intensive plastic deformation. Low Temp. Phys. 37(2):169-176. https://doi.org/10.1063/1.3540645

Williamson GK, Hall WH. (1953) X-ray line broadening from filed aluminium and wolfram. Acta Met. 1:22-31. https://doi.org/10.1016/0001-6160(53)90006-6

Williamson GK, Smallman RE (1956) III. Dislocation densities in some annealed and cold-worked metals from measurements on the X-ray Debye-Scherrer spectrum. Phil. Mag. 1:34-46. https://doi.org/10.1080/14786435608238074

Zhang Y, Wang Y, Zhang J (2020) Effect of grain size on shear banding in Ti-6Al-4V alloy. Metall. Mater. Trans. A51(12):6236-6248. https://doi.org/10.1007/s11661-020-05695-3